
CONDENSER AND DEAERATOR CONTROL USING FUZZY-NEURAL TECHNIQUE

Prof. Dr. Abduladhem A. Ali
Department of Computer Engg.

A'ayad Sh. Mohammed
Department of Electrical Engg.
College of Engineering, University of Basrah
Iraq

Abstract

A model reference adaptive control of condenser and deaerator of steam power plant is presented. A fuzzy-neural identification is constructed as an integral part of the fuzzy-neural controller. Both forward and inverse identification is presented.

In the controller implementation, the indirect controller with propagating the error through the fuzzy-neural identifier based on Back Propagating Through Time (BPTT) learning algorithm as well as inverse control structure are proposed.

Simulation results are achieved using Multi Input-Multi output (MIMO) type of fuzzy-neural network. Robustness of the plant is detected by including several tests and observations.

Keywords: Power plant control, Fuzzy neural, Condenser control, Dearator control, MIMO control.

I – Introduction

Because of the impertinence of the fundamental parts (condenser and deaerator) in completing the heat cycle and power generation in steam power plants, model reference adaptive control have been developed and implemented for controlling the condenser and the deaerator levels.

A simple control scheme such as PID controller can be used for such control. However, such controller is poor to overcome the disturbances that may occur on the plant working conditions.

Several types of controllers were presented to control the different parts of steam power plant, such as the twin turbine-generator system, including its associated control systems, performs satisfactorily in a variety of normal and energy operation modes [1]. In [2] a systematic method of choosing the frequency bias parameter and the integrator gain of the sampled data supplementary control using the discrete version of the Lyapunov's technique. Also the study presents data and control schemes for small and medium size boiler models [3].

Recently neurofuzzy model reference controller is adopted based boiler drum controller for power stations [4] Deaerator and condenser control have not been given the same attention..

II – Flow Diagram of the system under control

Figure (1) shows the flow diagram of the system under control. The circulating water (cooling water) is passing through the tubes of the condenser and receives energy from the steam that is coming from the Low Pressure Cylinder (LPC) of the turbine to the condenser by convection and conduction through the tube walls. The cooling water temperature is increased from its initial value (t_1) to a final value (t_2). The steam enters the condenser in a moist state, and its temperature remains constant through the condenser, but its latent energy is removed. Condensed steam, called (condensate), is collected in the hotwell, whose capacity should be equal to the maximum value of condensate produced.

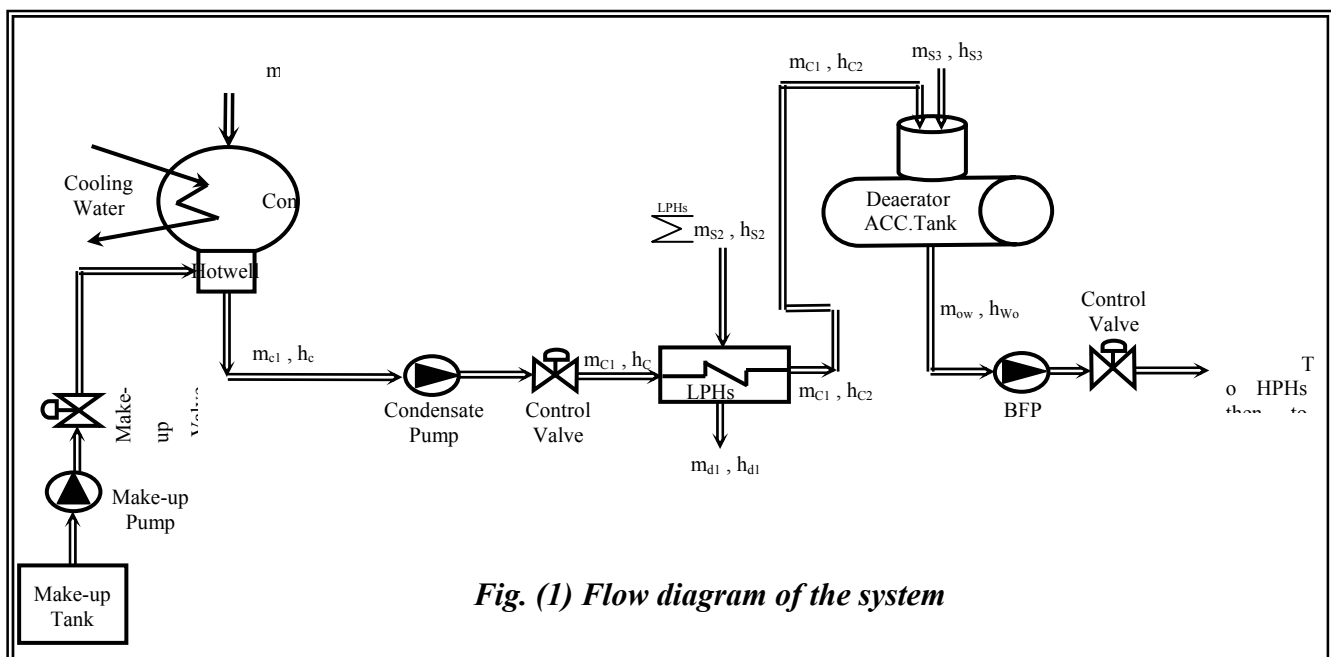


Fig. (1) Flow diagram of the system

Then condensate leaves the condenser by condensate pump and reaches the first stage of heating which is closed or surface type feed water heaters (Low Pressure Heaters LPHs). The water (condensate) passing through Low Pressure Heater tubes are surrounded by a steam coming from the Low Pressure Cylinder (LPC) of turbine. This steam is condensed in the heater tubes and then falls to the bottom of the heaters as a rain of drops. The heater drains then returned to the condenser through drain lines. The temperature of the condensate is raised and leaves the (LPHs) to the deaerator.

In the deaerator, the steam taken from (LPC) of the turbine and the condensate arrive from (LPHs) are mixed and all the non-condensable gases present in the mixture such

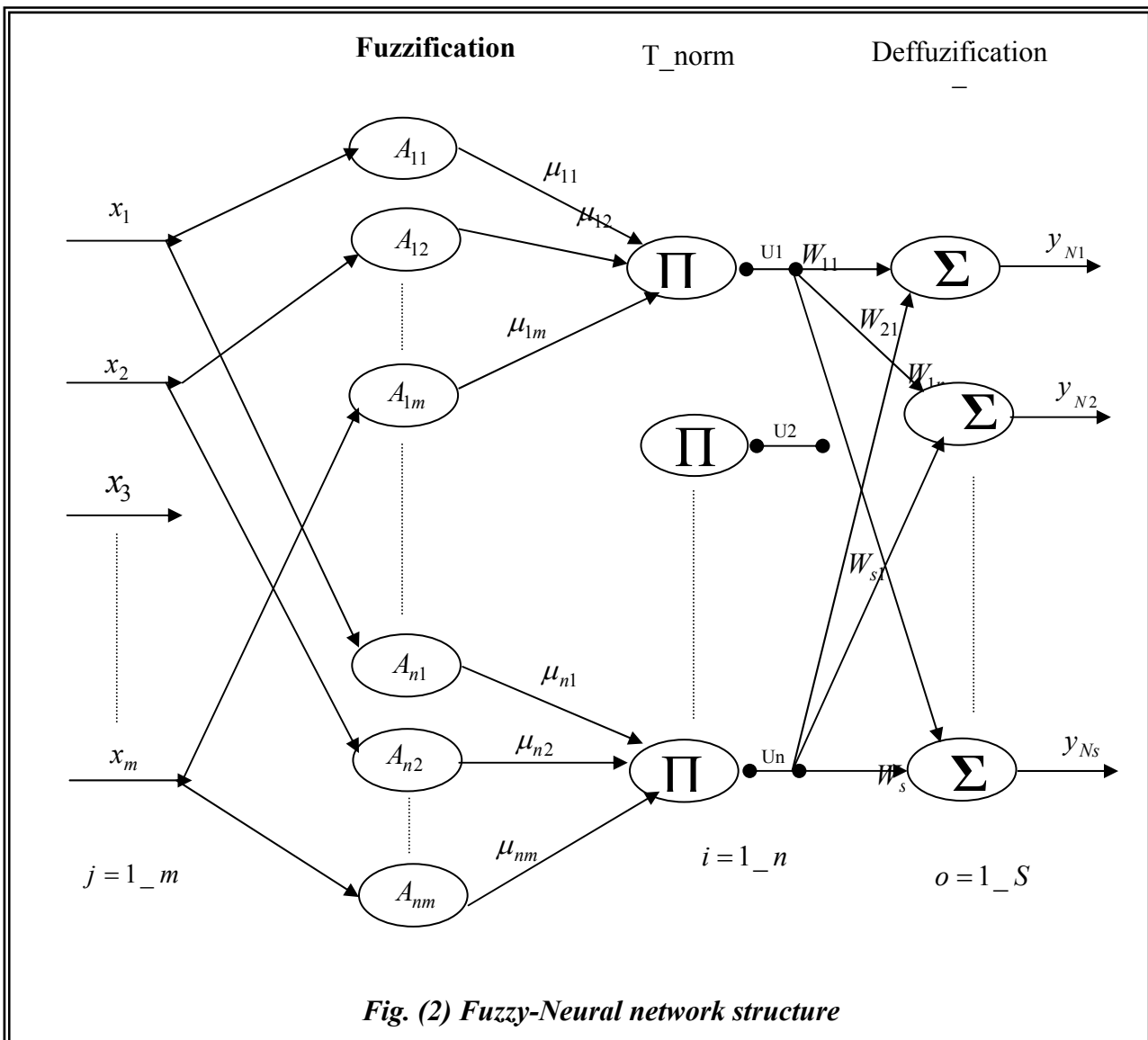
as (oxygen, carbon dioxide and ammonia) are removed. The feed water leaving the deaerator are forced to the Boiler Feed Pump (BFP) after passing through second stage of heating called High Pressure Heaters (HPHs).

Finally, the make-up tank are used to compensate the grow less of water (condensate) in the hotwell of the condenser.

More information about the parameters and dimensions of steam power plant that is listed in appendix.

III – Fuzzy-Neural Network Structure

The structure of a fuzzy-neural network with Multi Input and Multi Out- puts are represented in Fig. (2). This representation is a type of a feed forward neural network.



The first layer performs a fuzzification for each linguistic rule using Gaussian membership function, which is given in the following relation:

$$\mu_{ij}(x) = e^{-\frac{1}{2} \left(\frac{x_j - a_{ij}}{b_{ij}} \right)^2} \quad \dots(1)$$

where x_j is the j^{th} input variable, a_{ij} and b_{ij} are the center and width of the Gaussian membership function.

The outputs from this layer are fed to the next layer, which performs a T-norm operation (product operation) given by:

$$U_i = \prod_{j=1}^m \mu_{ij} \quad \dots(2)$$

where m is the number of input variables.

The last layer computes the overall outputs as the weighted sum of the incoming signals, to produce the center of gravity (COG) defuzzification operation, which can be obtained by the following equation:

$$y_{NS} = \sum_{i=1}^n u_i \cdot W_{si} \quad \dots(3)$$

where n is the number of rules, S is the number of outputs of fuzzy neural network.

Note that the adopted fuzzy-neural network here is modified to be unnormalized. A unnormalized fuzzy-neural network exhibits the desired performance for the identification and control of nonlinear systems. Moreover, there are two advantages of fuzzy-neural network with out a normalization process [5]:

1. A faster training rate than the one which is normalized.
2. A much simpler form of the input-output sensitivity equation than in a normalized of fuzzy-neural network.

Now, putting it all together, the outputs of fuzzy-neural network y_{NS} become:

$$y_{NS} = \sum_{i=1}^n W_{si} \cdot \left(\prod_{j=1}^m e^{-\frac{1}{2} \left(\frac{x_j - a_{ij}}{b_{ij}} \right)^2} \right) \quad \dots(4)$$

IV – Identification

The identification of dynamic behavior of the simulated model is done based on series-parallel fuzzy-neural networks.

Forward Identification

In this type, the inputs and outputs of the identifier network are the same inputs and outputs of the plant to be identified.

Single Multi Input-Multi Output (MIMO) network is implemented to identify the condenser level and the deaerator level simultaneously as shown in Fig. (3). This network has (10) inputs and (2) outputs.

The initial values of the membership function's centers are equally separated along the universe of discourse for all inputs. The width of all membership functions is equal to (0.28), and the initial values of weights are selected in the range between (0 and 3), and using the number of rules (50 Rules). A gradient decent based back-propagation algorithm is employed to adjust the parameters of the (MIMO) fuzzy-neural network by using the training pattern.

In this case, the adaptation of weights for condenser level (w_{1i}) and deaerator level (w_{2i}) are effected by the errors in each outputs separately while the adaptation of centers (a_{ij}) and width (b_{ij}) are effected by the errors in both outputs, i.e.:

The main goal of supervised learning algorithm is to minimize the error function:

$$E_T = \frac{1}{2} E_1^2 + \frac{1}{2} E_2^2 \quad \dots(5)$$

$$E = \frac{1}{2} (y_{N1}(k) - y_{p1}(k))^2 + \frac{1}{2} (y_{N2}(k) - y_{p2}(k))^2 \quad \dots(6)$$

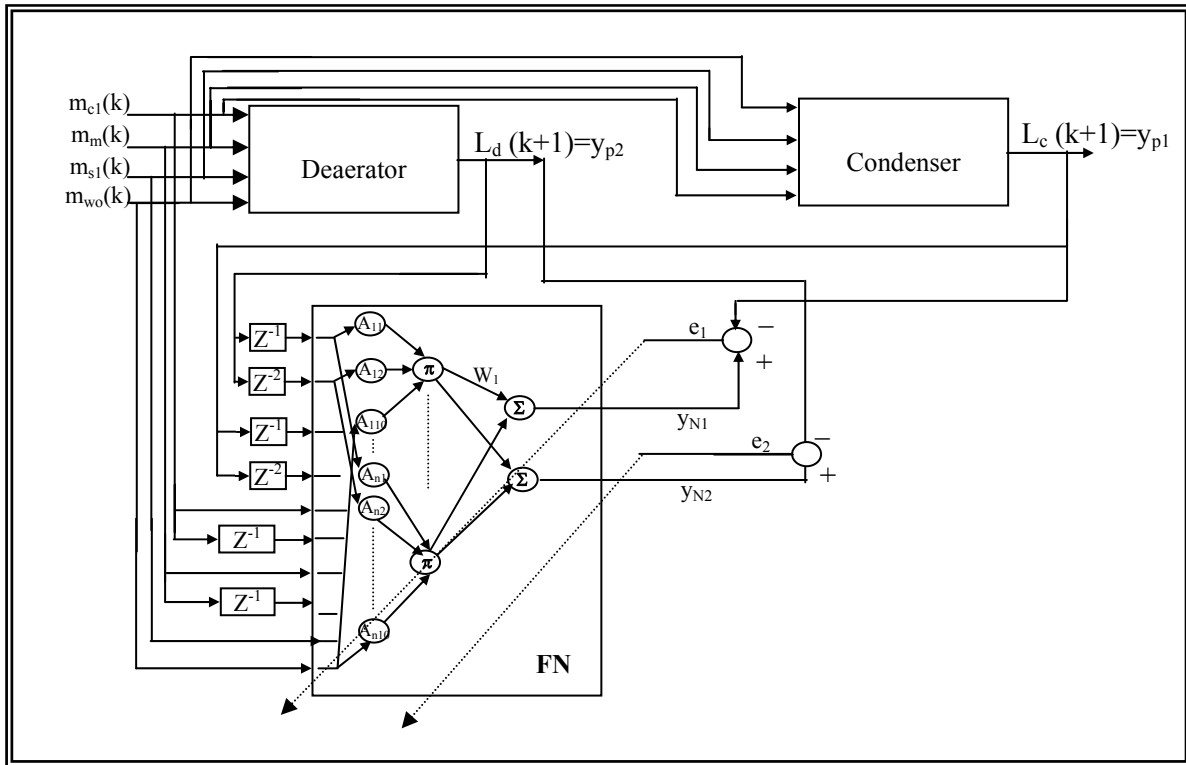


Fig. (3) Construction of single (MIMO) forward identification network

where $y_{N1}(k), y_{N2}(k)$ are the output1 and the output2 of fuzzy-neural network respectively and $y_{p1}(k), y_{p2}(k)$ are the desired outputs (condenser level and deaerator level respectively) for the j^{th} input pattern.

The gradient descent algorithm gives the following iterative equations for the parameter values:

$$a_{ij}(k+1) = a_{ij}(k) - \zeta_{a_{ij}} \frac{\partial E_T}{\partial a_{ij}} \quad \dots(7)$$

$$b_{ij}(k+1) = b_{ij}(k) - \zeta_{b_{ij}} \frac{\partial E_T}{\partial b_{ij}} \quad \dots(8)$$

$$w_{i1}(k+1) = w_{i1}(k) - \zeta_{w_{i1}} \frac{\partial E_T}{\partial w_{i1}} \quad \dots(9)$$

$$w_{i2}(k+1) = w_{i2}(k) - \zeta_{w_{i2}} \frac{\partial E_T}{\partial w_{i2}} \quad \dots(10)$$

where ζ is the learning rate for each parameter in the system, $i=1,2,\dots,n$ and $j=1,2,\dots,m$.

Taking the partial derivative of the error function given by eqn. (6), we can get the following equations:

$$\frac{\partial E_T}{\partial a_{ij}} = E_1 \frac{\partial E_1}{\partial a_{ij}} + E_2 \frac{\partial E_2}{\partial a_{ij}} \quad \dots(11)$$

$$\frac{\partial E_T}{\partial b_{ij}} = E_1 \frac{\partial E_1}{\partial b_{ij}} + E_2 \frac{\partial E_2}{\partial b_{ij}} \quad \dots(12)$$

$$\frac{\partial E_T}{\partial w_{i1}} = E_1 \frac{\partial E_1}{\partial w_{i1}} + E_2 \frac{\partial E_2}{\partial w_{i1}} \quad \dots(13)$$

$$\frac{\partial E_T}{\partial w_{i2}} = E_1 \frac{\partial E_1}{\partial w_{i2}} + E_2 \frac{\partial E_2}{\partial w_{i2}} \quad \dots(14)$$

Hence, the new value of a_{ij} after adaptation is equal to:

$$a_{ij}(k+1) = a_{ij}(k) - \zeta_{a_{ij}} [(y_{N1} - y_{P1})w_{1i} + (y_{N2} - y_{P2})w_{2i}] u_i \frac{(x_j - a_{ij})}{(b_{ij})^2} \quad \dots(15)$$

Similarly, $b_{ij}(k+1)$, $w_{i1}(k+1)$ and $w_{i2}(k+1)$ could be obtained from the following equations:

$$b_{ij}(k+1) = b_{ij}(k) - \zeta_{bij}[(y_{N1} - y_{P1})w_{i1} + (y_{N2} - y_{P2})w_{i2}]u_i \frac{(x_j - a_{ij})^2}{(b_{ij})^3} \quad \dots(16)$$

$$w_{i1}(k+1) = w_{i1}(k) - \zeta_{w_{i1}}(y_{N1} - y_{P1})u_i \quad \dots(17)$$

$$w_{i2}(k+1) = w_{i2}(k) - \zeta_{w_{i2}}(y_{N2} - y_{P2})u_i \quad \dots(18)$$

According to the information and after the execution of (10) iterations of learning algorithm shown in Equations (15) to (18) the responses of this part are shown in Figs. (4)-(6). First steps of training of condenser level and deaerator level of the forward identification are observed in Fig. (4), where Fig. (4.a) and Fig. (4.b) represent responses of both levels respectively and also their corresponding identifier outputs.

Parameters update was continued for (10) iterations, till convergence of the total square of error $E_T(k)$ towards zero is satisfied, as illustrated in Fig. (5.a). Parameters updating progress is presented in Fig. (5.b) for (3) randomly selected parameters. Therefore, the end of adaptation was reached by arriving the parameters to their steady state values.

Figure (6.a) and Fig. (6.b) shows the actual outputs and identifier outputs of both condenser and deaerator respectively after the end of adaptation.

Two values for the level set-point (Lref) are employed to test the learned identifier, these values selected as: one is the minimum value of levels and the other is a maximum value of levels, ($L_{ref\ 1\ min}=0.5$ m and $L_{ref\ 1\ max}=1.0$ m for condenser), ($L_{ref\ 2\ min}=1.5$ m and $L_{ref\ 2\ max}=2.2$ m for deaerator) and they are applied successively. These values have been used because it reflects all the region of interest. Therefore, the curves in Fig.(6) reveal how the fuzzy-neural identifiers

learned the dynamic of the condenser and the deaerator.

Inverse Identification

The structure of a fuzzy-neural network with Multi Input and Multi Outputs are similar to that used in the forward identification the main difference is in the inputs and outputs of the network. The input to the fuzzy-neural Network inverse identifier is the output of the plant, while the output of the network is the input of the plant.

Single (MIMO) network has (10) inputs and (2) outputs used to identify the two inputs of the plant: condensate flow rate (\dot{m}_{c1}) and make-up water (\dot{m}_m) instantaneously as shown in Fig (7). The number of rules used are 50 rules.

Adaptation of this system has been continued for (25) iterations until convergence of the total squared error $E_T(k)$ towards zero has been reached. Fig. (8.a) show the first learning period of condensate flow rate and its coincidence to the actual input (\dot{m}_{c1}), while Fig. (8.b) illustrates the corresponding curves of the make-up water (\dot{m}_m) and its identifier for first learning period. Responses of the squared error and development of (3) selected parameters are observed in Figs. (9.a) and (9.b) respectively, and the curves reveal how updating is complete when the parameters reached their steady state values. Figs. (10.a) and (10.b) represent the condensate flow rate (\dot{m}_{c1}) and its identifier and make-up water (\dot{m}_m) and its identifier at the end of adaptation period respectively.

V – Control

The purpose of designing a controller is to control the condensate valve and make-up valve, which generate the desired control inputs (\dot{m}_{c1} and \dot{m}_m) receptively. The simulation results depend on the dynamic model of the condenser and the deaerator is based on the conservation of mass and energy balance principal. The final objective is that

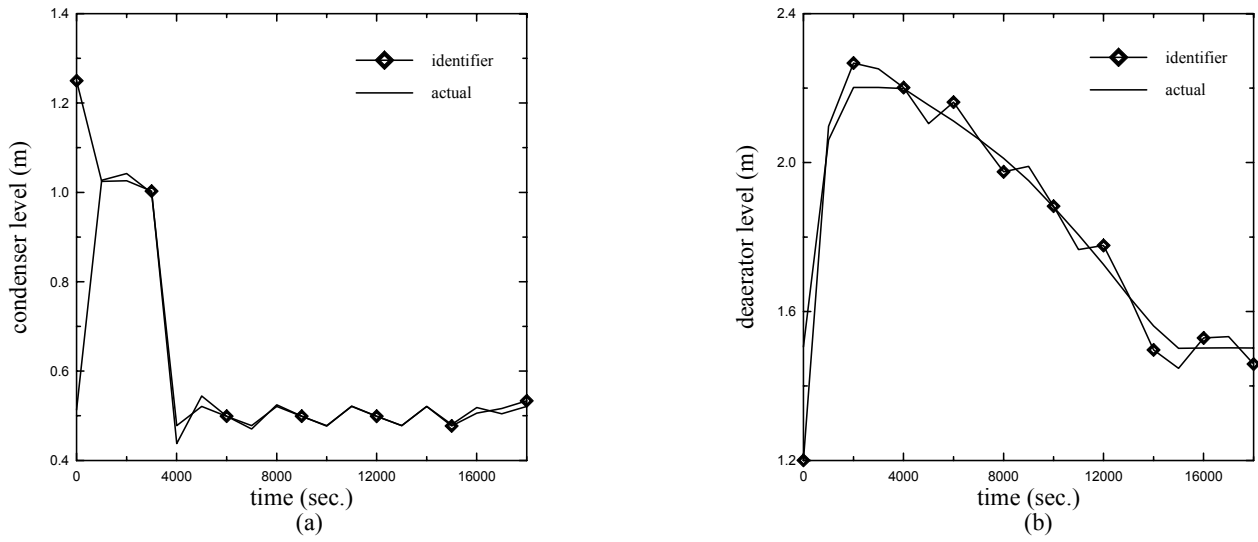


Fig. (4) First steps of plant forward identification [MIMO network]

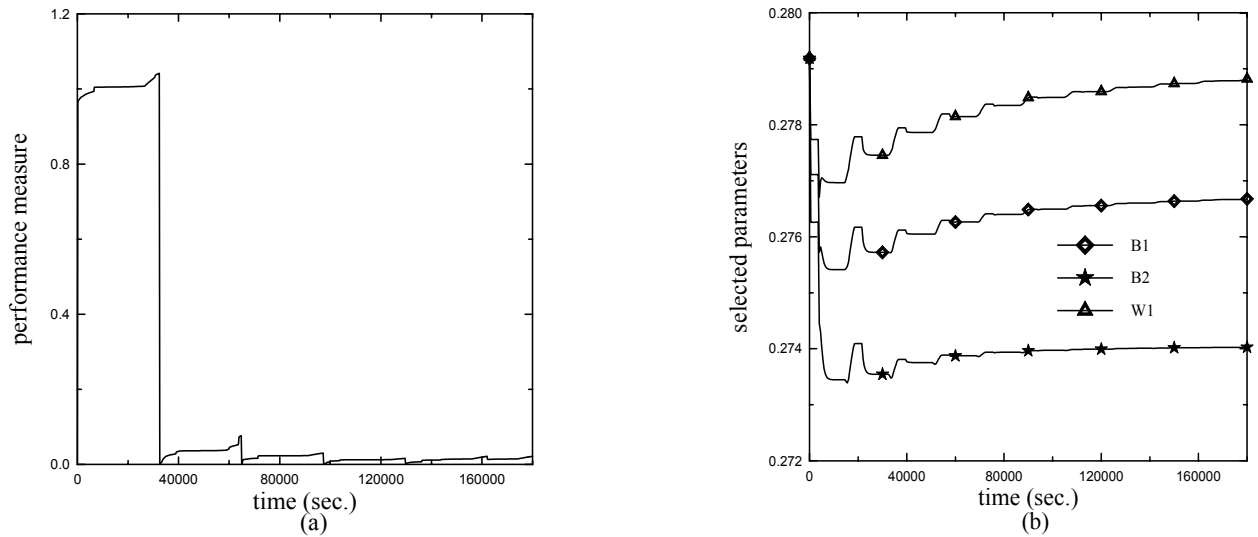


Fig. (5) Learning progress of the plant forward identification [MIMO network]

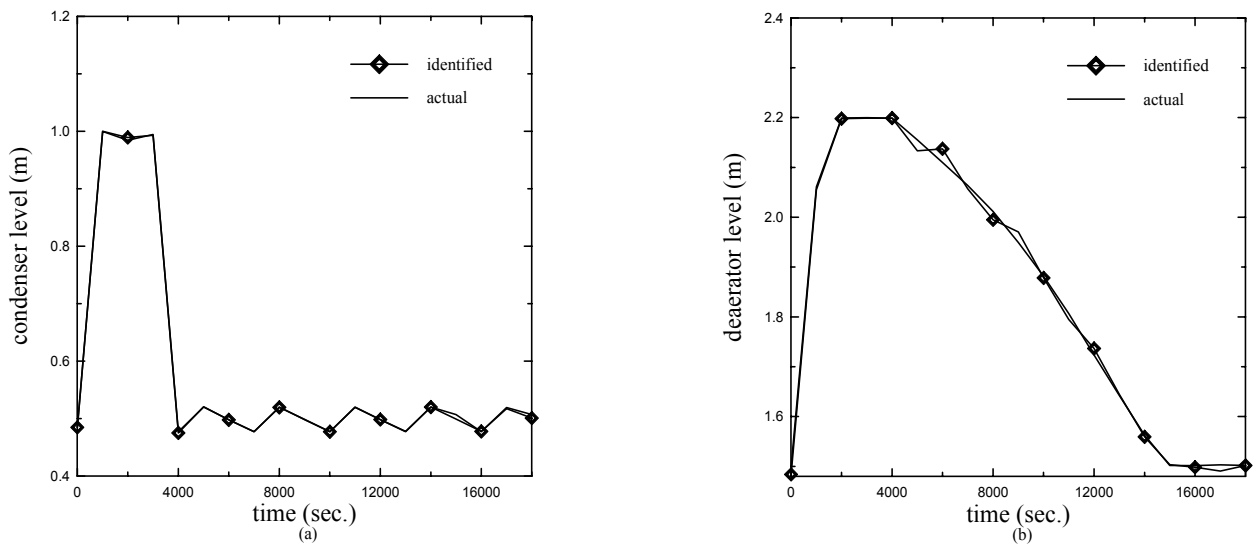


Fig. (6) Last steps of plant forward identification [MIMO network]

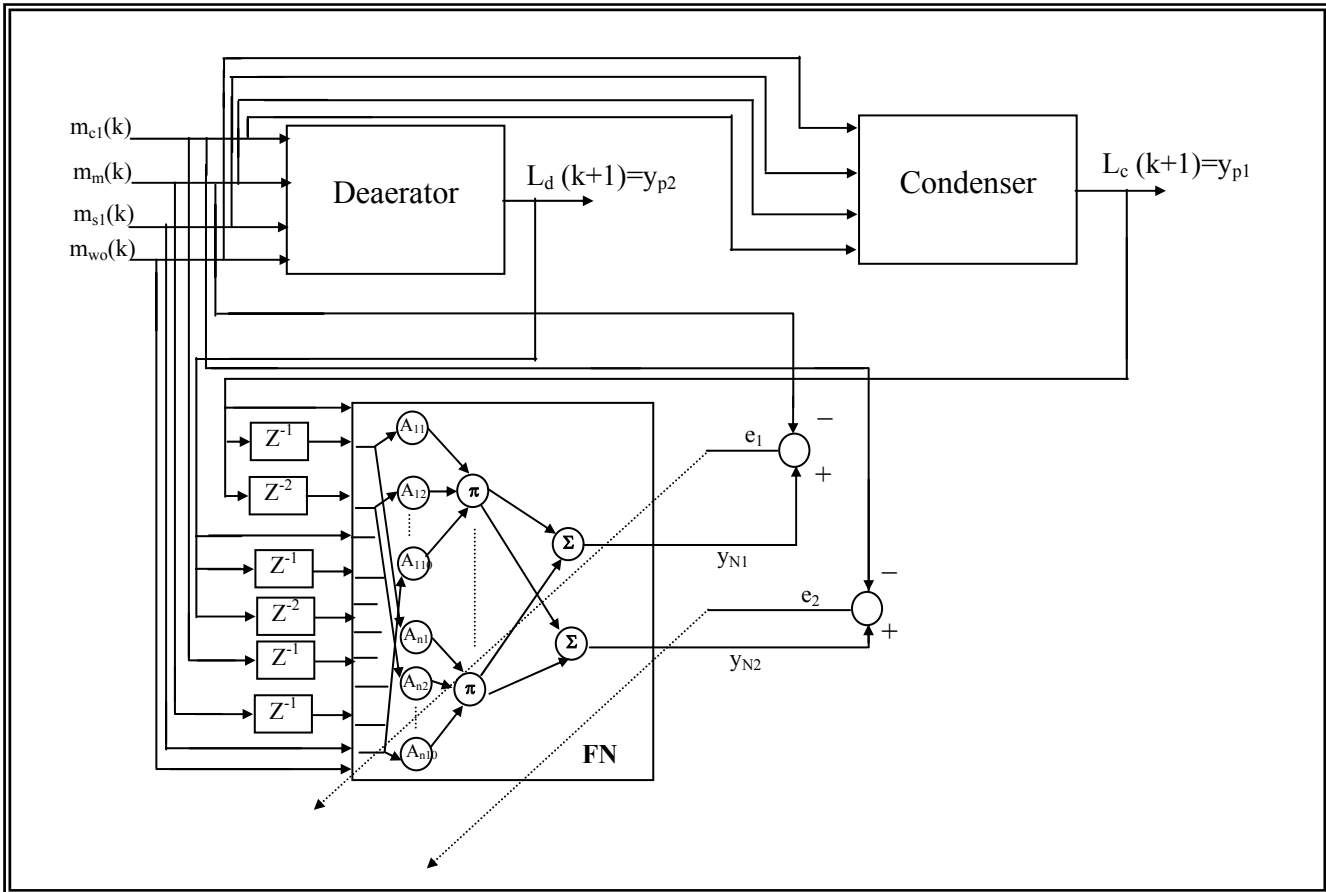


Fig. (7) Construction of single (MIMO) inverse identification network

the condenser level and the deaerator level must tracks a desired reference model, such that the performance of plant outputs is controlled.

The designed reference model has the same properties of the plant. The model can be described by the following equations.

$$YR_1 = YR_0 + T \frac{(\dot{m}_{s1r} - \dot{m}_{c1r} + \dot{m}_{m_r} + \dot{m}_{d1r} + \dot{m}_{D_r})}{\rho_{c1r} a_{hr}} \quad \dots(19)$$

$$e_c = YR_1 - Lref_1 \quad \dots(20)$$

$$u_{12cr} = \begin{cases} 0 & \text{if } (e_c < 0.5) \\ 1 & \text{if } (e_c > 0) \\ \exp(100 * e_c) & \text{if } (-0.5 < e_c < 0) \end{cases} \quad \dots(21)$$

$$\dot{m}_{c1r} = 85.861 * \sqrt{\frac{(\frac{C_{v1r}}{C_{R1r}})^2 + 1}{(\frac{C_{v1r}}{C_{R1r}})^2 + \frac{1}{(u_{12cr})^2}}} \quad \dots(22)$$

$$A_{accr} = \frac{V_{accr} + T(\dot{m}_{s3r} + \dot{m}_{c1r} - \dot{m}_{wor} + \dot{m}_{d2r})/(\rho_{wor})}{L_{accr}} \quad \dots(23)$$

$$\theta_r = 14.0567 + 262.63A_{accr} - 422.987A_{accr}^2 + 390.427A_{accr}^3 - 204.333A_{accr}^4 + 64.2516A_{accr}^5 - 12.5197A_{accr}^6 + 1.51415A_{accr}^7 - 0.109777A_{accr}^8 + 0.00432412A_{accr}^9 - 7.00254E - 0.005A_{accr}^{10} \quad \dots(24)$$

$$YR_2 = 2 * r_{accr} * \sin^2\left(\frac{1}{4}\theta_r\right) \quad \dots(25)$$

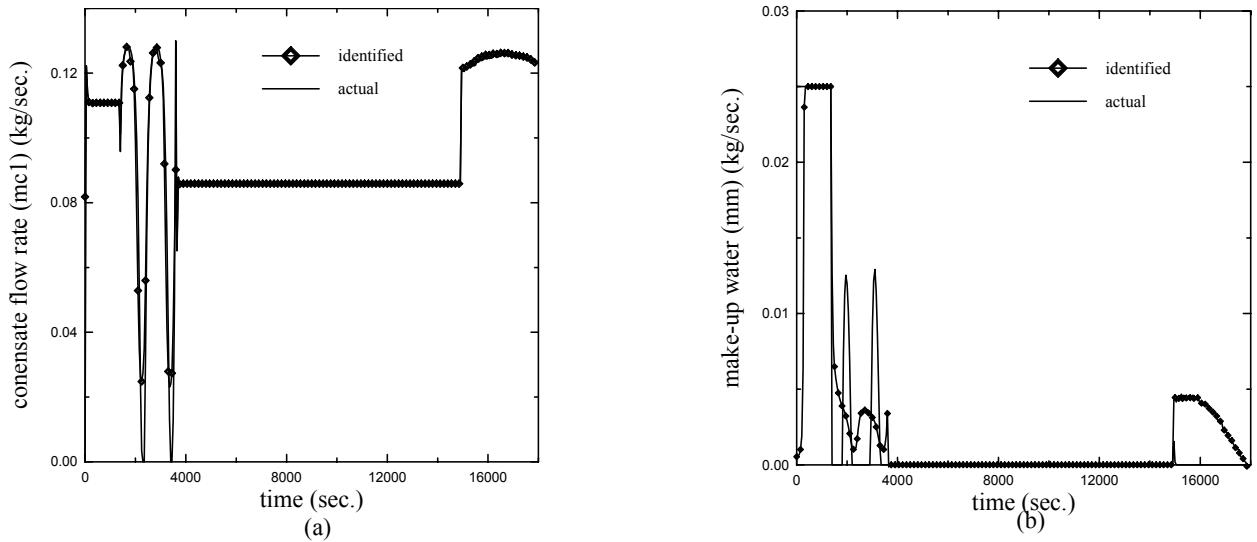


Fig. (8) First steps of plant inverse identification [MIMO network]

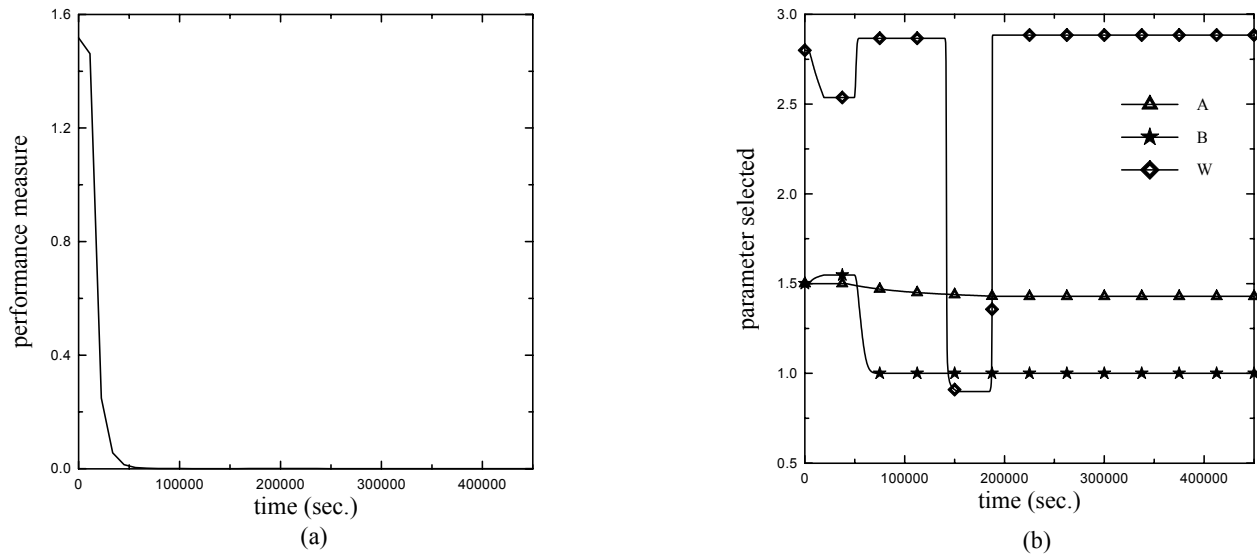


Fig. (9) Learning progress of the plant inverse identification [MIMO network]

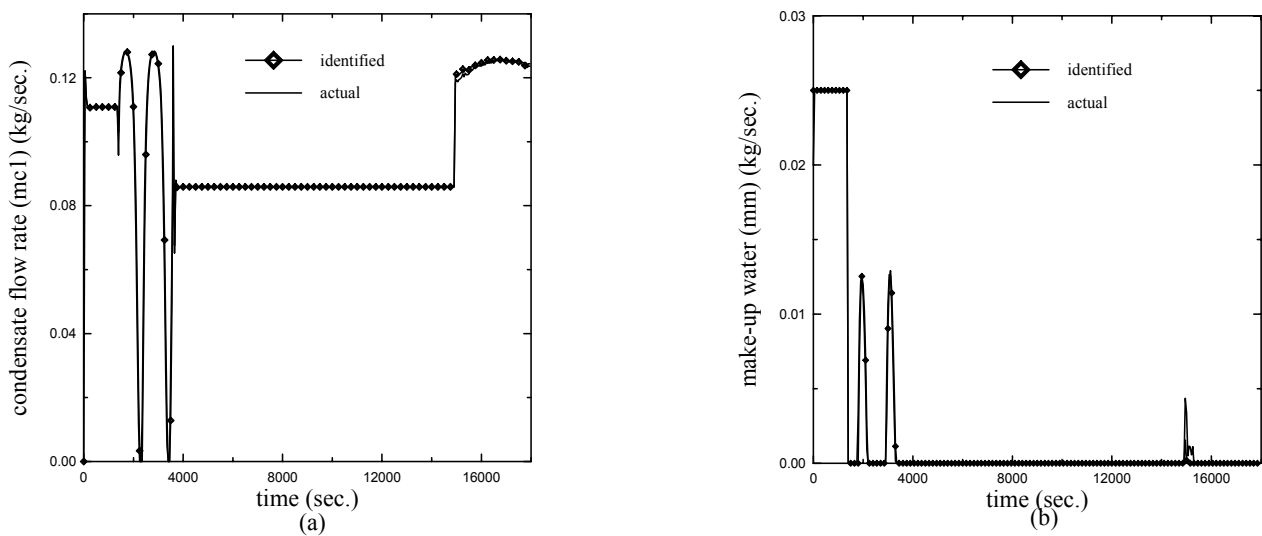


Fig. (10) Responses after inverse identification complete [MIMO network]

$$ed = Lref_2 - YR_2 \quad \dots(26)$$

$$u_{12dr} = \begin{cases} 0 & \text{if } (e_d > 0.7) \\ 1 & \text{if } (e_d < 0) \\ \exp(-e_d) & \text{if } (0 < e_d < 0.7) \end{cases} \quad \dots(27)$$

$$\dot{m}_{mr} = 16.667 * \sqrt{\frac{\left(\frac{C_{v2r}}{C_{R2r}}\right)^2 + 1}{\left(\frac{C_{v2r}}{C_{R2r}}\right)^2 + \frac{1}{(u_{12dr})^2}}} \quad \dots\dots\dots(28)$$

where

$YR_1, YR_2, \dot{m}_{slr}, \dot{m}_{clr}, \dot{m}_{mr}, \dots, r_{accr}$ and \dot{m}_{wor} are the corresponding parameters of the condenser and the deaerator, $Lref1$ and $Lref2$ are the condenser level set point and the deaerator level set pint respectively.

Parameter values of the reference model are listed in appendix.

Indirect Fuzzy-Neural Control

We used (MIMO) fuzzy-neural identifier in the (MIMO) indirect controller method as a path for the output error propagation to the fuzzy-neural controller as shown in Fig. (11). In this type of control, two fuzzy-neural networks, fuzzy-neural network identifier and controller is employed, abbreviated by FNNI and FNNC respectively.

The controller network learning is based on the plant sensitivity (gradient of the output with respect to its input) which can be described as follows:

$E_c(k)$ is the total squared error of the difference between the reference output $y_r(k)$ and the plant output $y_p(k)$ is defined as:

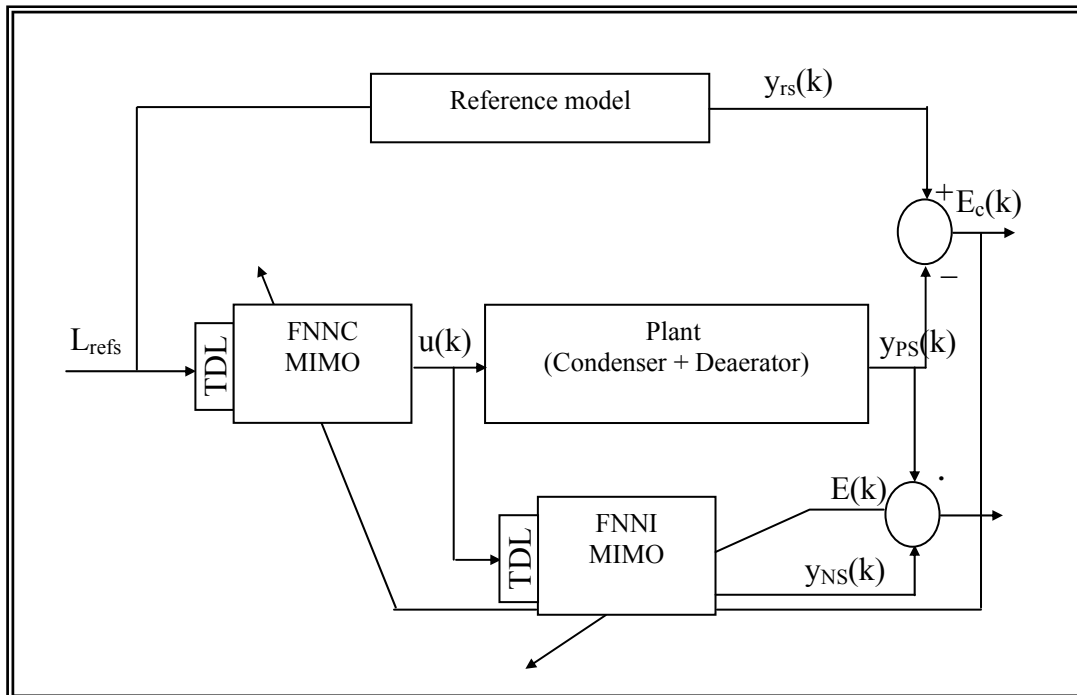


Fig. (11) Indirect Fuzzy-neural controller

$$E_c(k) = \frac{1}{2} \sum_{s=1}^o (y_{rs}(k) - y_{ps}(k))^2 \quad \dots(29)$$

where, o : is the number of plant outputs.

The gradient decent algorithm used to adjust arbitrary parameter of the fuzzy-neural controller as follows:

$$\theta(k+1) = \theta(k) - \zeta_{\theta} \frac{\partial E_c(k)}{\partial \theta} \quad \dots(30)$$

where, ζ_{θ} : is the learning rate of that parameter.

Then the gradient of error with respect to an arbitrary parameter θ is:

$$\begin{aligned} \frac{\partial E_c(k)}{\partial \theta(k)} &= - \sum_{s=1}^o (y_{rs}(k) - y_{ps}(k)) \cdot \frac{\partial y_{ps}(k)}{\partial \theta(k)} \\ &= - \sum_{s=1}^o (y_{rs}(k) - y_{ps}(k)) \cdot \frac{\partial y_{ps}(k)}{\partial u(k)} \cdot \frac{\partial u(k)}{\partial \theta(k)} \end{aligned} \quad \dots(31)$$

where, $\frac{\partial y_{ps}(k)}{\partial u(k)}$: is called the plant sensitivity,

$u(k)$: is the input vector of the plant inputs,

$$u(k) = \begin{bmatrix} u_1(k) \\ u_2(k) \\ \vdots \\ u_m(k) \end{bmatrix},$$

m : is the number of input variables.

Then,

$$\left. \frac{\partial y_{ps}(k)}{\partial u(k)} \right|_{fors=1} = \begin{bmatrix} \frac{\partial y_{p1}(k)}{\partial u_1(k)} & \frac{\partial y_{p1}(k)}{\partial u_2(k)} & \dots & \frac{\partial y_{p1}(k)}{\partial u_m(k)} \end{bmatrix} \quad \dots(32)$$

and,

$$\frac{\partial u(k)}{\partial \theta(k)} = \begin{bmatrix} \frac{\partial u_1(k)}{\partial \theta(k)} \\ \frac{\partial u_2(k)}{\partial \theta(k)} \\ \vdots \\ \frac{\partial u_m(k)}{\partial \theta(k)} \end{bmatrix}_{[m*1]} \quad \dots(33)$$

But $\frac{\partial y_{ps}(k)}{\partial u(k)}$ cannot be obtained

unless a complete knowledge about the plant is required, due to the high nonlinear elements contained. Therefore the plant sensitivity was replaced by sensitivity model of the plant forward identifier based on a novel method was derived in [6] which is used as a path to propagate error to the fuzzy-neural controller.

The sensitivity model is:

$$\frac{\partial y_{ps}(k)}{\partial u(k)} = \frac{\partial y_{Ns}(k)}{\partial u(k)} \quad \dots(34)$$

In this paper, the plant consists of two inputs (i.e., $u(k) = \begin{bmatrix} \dot{m}_{c1} \\ \dot{m}_m \end{bmatrix}$), and two outputs (i.e., $y_p(k) = [y_{p1}(k) y_{p2}(k)]$). And (MIMO) fuzzy-neural controller has (12) inputs and (2) output and 60 Rules.

The initial values of the membership function's centers are equally separated along the universe of discourse of all inputs. The width of all membership functions is equal to (0.28), and the initial values of weights are selected in the range between (0 and 3).

After using the above information and all learning algorithms shown in eqns. (29 to 34) with two step- reference levels, which are ($L_{ref 1 \min}=0.5m$, $L_{ref 1 \max}=1.0m$ for condenser level) and ($L_{ref 2 \min}=1.5m$, $L_{ref 2 \max}= 2.2m$ for deaerator level), the first steps of the learning period of the fuzzy-neural controller action are illustrated in Fig. (12). Figure (12.a) represents the condenser level (the actual and

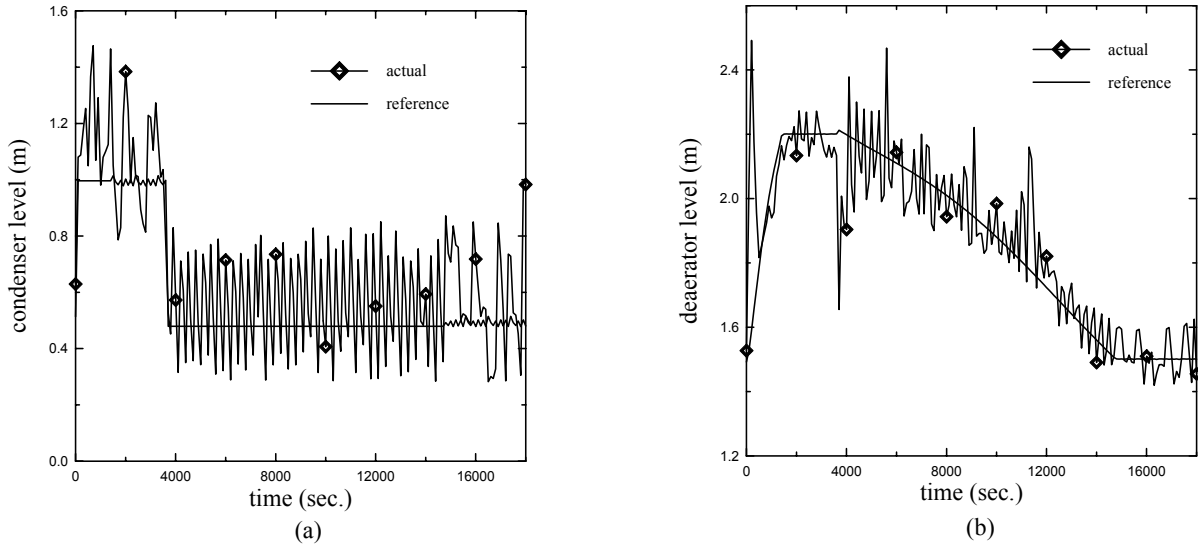


Fig. (12) First steps learning of indirect fuzzy-neural controller [MIMO network]

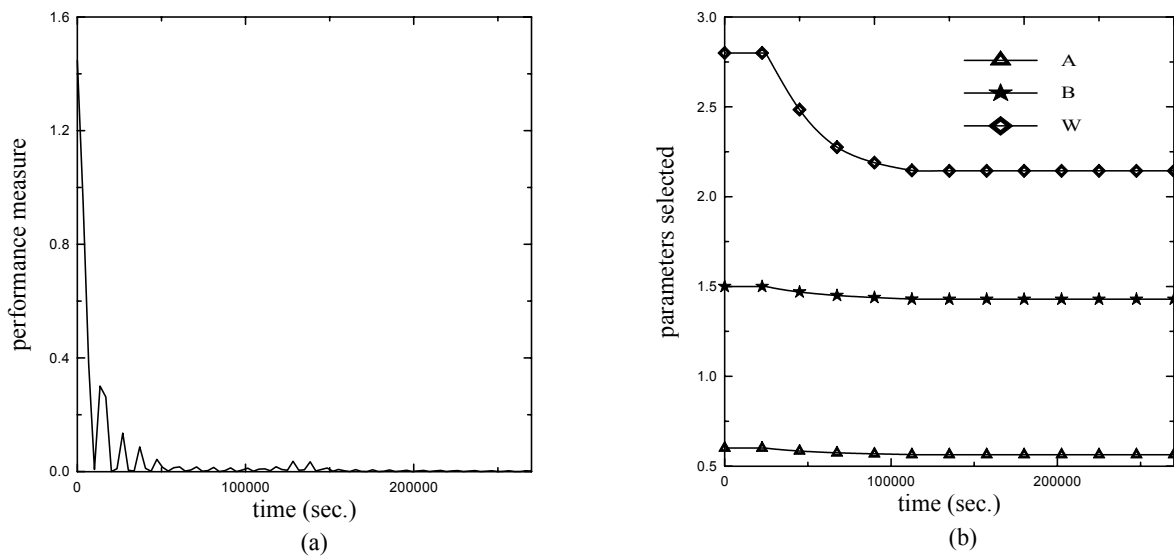


Fig. (13) Learning progress of indirect fuzzy-neural controller [MIMO network]

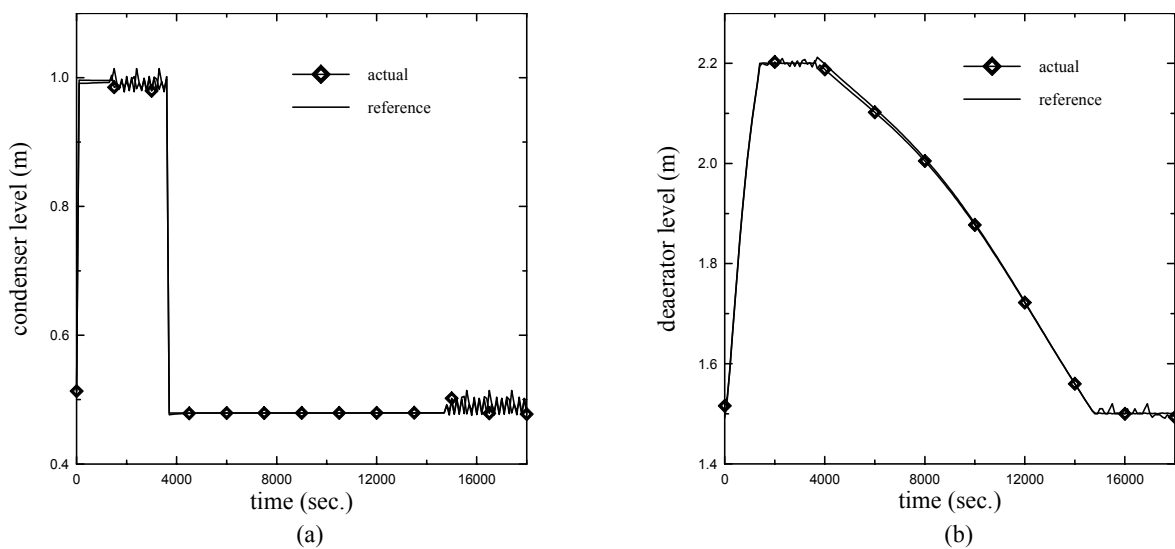


Fig. (14) Last steps learning of indirect fuzzy-neural controller [MIMO network]

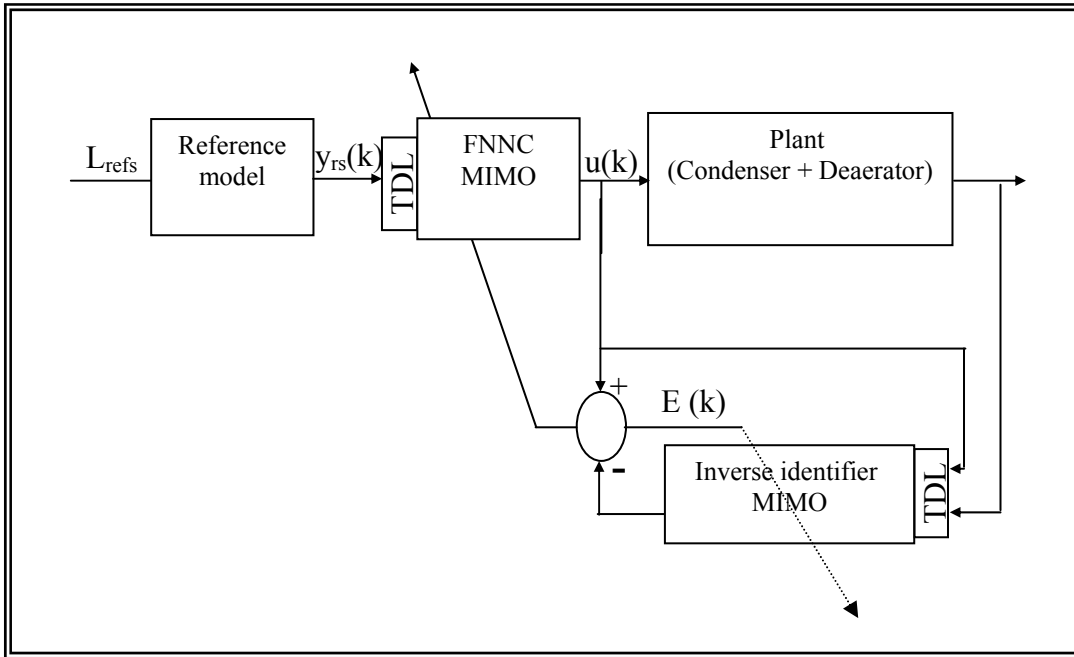


Fig.(15) The Inverse Controller

the reference). Deaerator level is observed in Fig. (12.b). Training was continued for (15) step inputs till convergence of the squared error $E_c(k)$ towards zero is satisfied. Fig. (13.a) illustrates the error convergence, while Fig. (13.b) represents the development of (3) selected parameters of the proposed fuzzy-neural controller until they reach their steady-state values. After learning is complete the responses of levels of the condenser and the deaerator are shown in Fig. (14), and this figure represent a good performance for the fuzzy-neural control proposed.

Inverse Control

In this work, we use the (MIMO) inverse identifier network that discussed in sec. (IV) as a controller, because this method is simpler in generating the desired input for the plant (\dot{m}_{cl} and \dot{m}_m) and does not requires further training.

After the learning period completes, the inverse identifier has the inverse dynamics of the condenser and deaerator. Therefore, the outputs of the controller are utilized as inputs to the plant, where the levels of condenser and

deaerator are to track to the reference model outputs. The outputs of the reference model are utilized as inputs to the controller (inverse identifier) as shown in Fig (14).

This type of controller can be understood easily if we assume that if the plant is linear. In which is this case, the identifier identifies the inverse transfer function $G^{-1}(s)$.

If the identified model is placed before the plant, and its input is generated for the reference model $M(s)$ then the resulting transfer function:

$$\frac{Y(s)}{I_{ref}} = M(s) \cdot G^{-1}(s) \cdot G(s) = M(s) \quad \dots(12)$$

Therefore the output of the plant is guaranteed to track the reference model output as shown in Fig. (16).

VI- Disturbance Effects

To check robustness of the proposed controller, several disturbances are applied to the plant, as shown in Figs. (17 to 19):

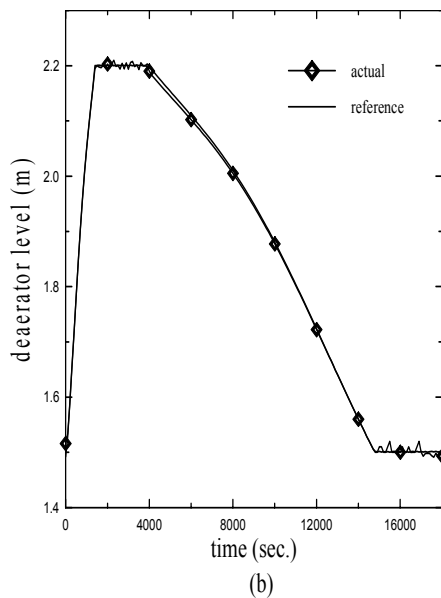
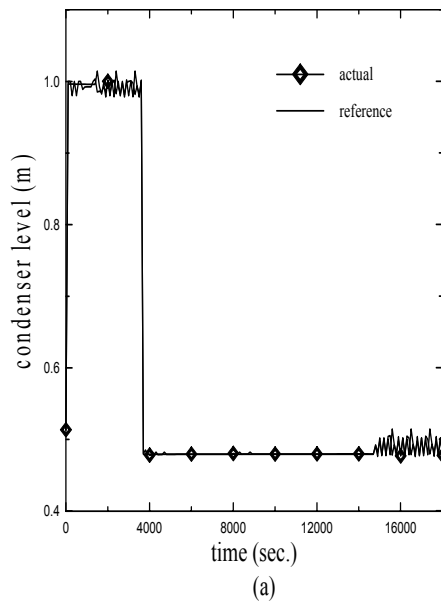


Fig.(16) Response of the Inverse Controller

1. Steam flow from (LPC) of the turbine to the condenser (\dot{m}_{c1}) is changed from (100% load) to (40% load) at time (2200 sec.). As shown from Fig. (16) (for indirect fuzzy neural, inverse fuzzy neural and PI controllers) the deaerator level and its valve opening (o_2) which are decreased too for a period of time a bout (150 sec.) and there return back to their reference values.
2. Figure. (17) shows responses of the condenser level and its valve opening when

fault occurs in the (LPH_s) and hence, removed from the system.

3. Finally, feed water flow rate (\dot{m}_{wo}) extracted from the deaerator was changed to (70%), and Fig. (18) illustrate the effect of disturbance on the deaerator level and its valve opening for the two types of controllers.

For the purpose of comparison the following disturbances results that are applied to the plant using the fuzzy-neural controller and the results when using the conventional controller, we observed that fuzzy-neural controller is less effected by there disturbances than conventional controller; so, the fuzzy-neural controllers are more robust than conventional controllers.

VII- Conclusions

A fuzzy-neural model reference adaptive control structure is presented and used for controlling the condenser level and the deaerator level of steam power plant. A fuzzy-neural network is constructed for both the identifier and the controller. A simulation results shows good performance for proposed scheme.

VIII- References

- [1] H. G. Kwatny and K. C. Kalnitsy, " Turbine-Generator System Control For a HTGR Power Plant", Automatica, vol. 6, PP. 265_279, Printed In Great Britain, Pergainon Press Ltd. 1980.
- [2] S. C. Tripathy, C. S. Jha and G. S. Hope," Sampled Data Automatic Generation Control Analysis With Reheat Steam Turbines And Governor Dead-Band Effects", IEEE Transactions On Power Apparatus and Systems, vol. PAS_103, No. 5, May 1984.
- [3] E. Cheres, " Small and Medium Size Drum Boiler Models Suitable for Long Term Dynamic Response", IEEE Transactions on Energy Conversion, vol. 5, no. 4, December 1990.

[4] Ali F. Marhoon, “ Neurofuzzy Based Boiler Drum Controller for Power Stations”, Ph. D. Thesis, University of Basrah, Feb. 2002.

[5] Cornelius T. Leondes, “ Fuzzy Logic and Expert Systems Applications”, Neural Network Systems Techniques and Applications, 1998.

[6] G. Light Body and G. W. Irwin, “Nonlinear Control Structures Based on Embedded Neural System Models”, IEEE Transactions on Neural Networks, vol. 8, no. 3, May 1997.

[7] Data Sheets of the Condenser and the Deaerator of *AL-Najeebiah* power plant references

Appendix A

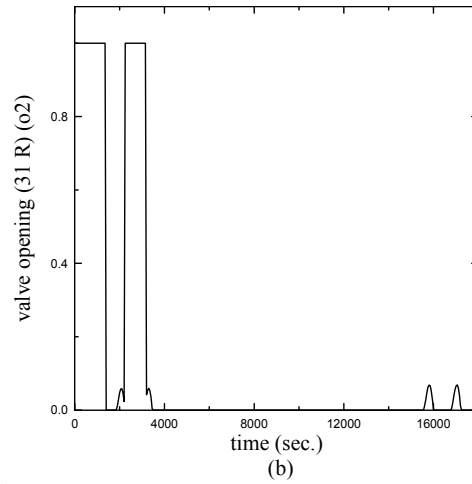
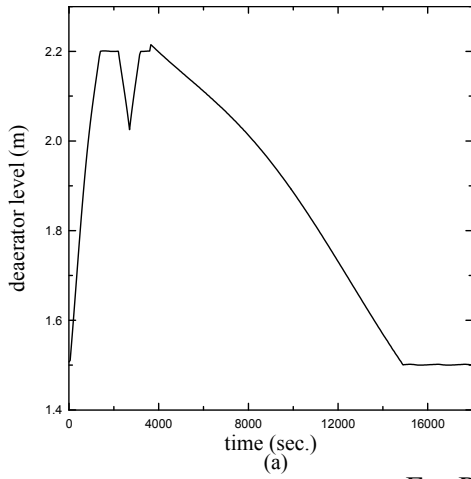
Physical Dimensions of *AL_Najeebiah* Power Plant [7]

\dot{m}_{s1}	71.75	Kg/sec.	$\sum^{LPH_s} \dot{m}_{s2}$	35467.99	KJ/sec.
h_{s1}	2565.4	KJ/Kg	h_c	170.82144	KJ/Kg
h_{c1}	146.12	KJ/Kg	h_{d1}	179.07	KJ/Kg
h_{fg}	2419.28	KJ/Kg	\dot{m}_{s3}	4.69444	Kg/sec.
\dot{m}_{d1}	13.5	Kg/sec.	h_{s3}	2983.095	KJ/Kg
\dot{m}_D	0.61111	Kg/sec.	\dot{m}_{wo}	105.591	Kg/sec.
ρ_{c1}	1000	Kg/m ³	h_{wo}	678.68	KJ/Kg
a_h	2	m ²	\dot{m}_{d2}	12.75	Kg/sec.
\dot{v}_{co}	0.085861	m ³ /sec.	h_{d2}	672.8	KJ/Kg
c_{v1}	0.006	—	ρ_{wo}	1000	Kg/m ³
c_{R1}	0.002354	—	ρ_m	1000	Kg/m ³
c_{v2}	0.0011	—	L_{acc}	13.5	m
c_{R2}	0.000134	—	r_{acc}	1.75	m
$o_1 \& o_2$	0 — 1	—	\dot{v}_{mo}	0.016667	m ³ /sec

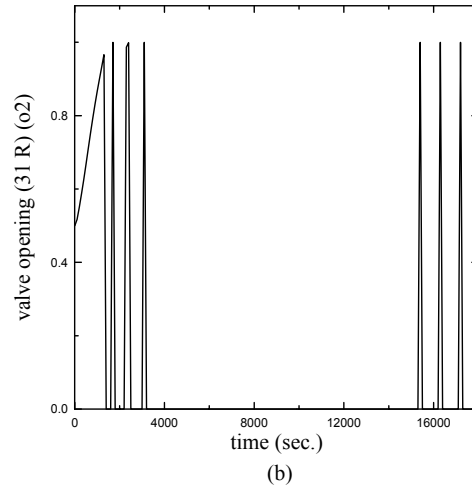
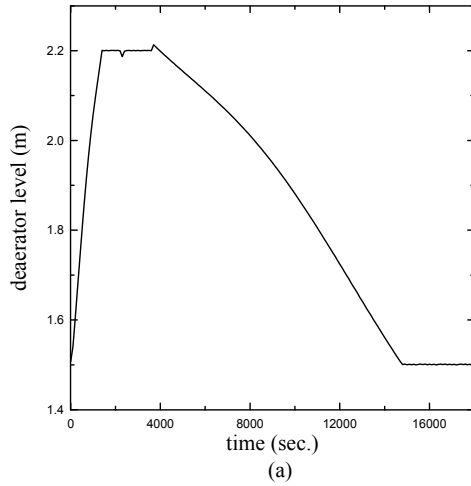
Appendix B

(b) Parameters of Reference Model:

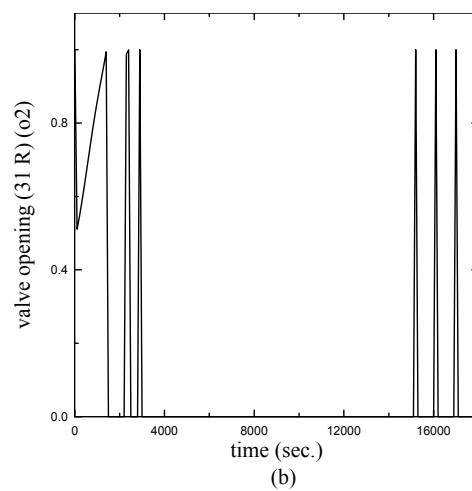
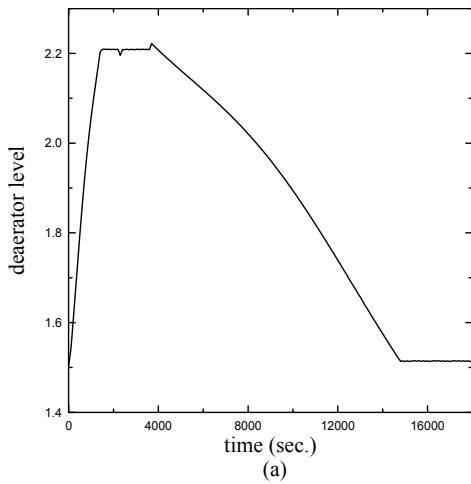
\dot{m}_{s1r}	71.75	Kg/sec.
\dot{m}_{d1r}	13.5	Kg/sec.
\dot{m}_D	0.61111	Kg/sec.
ρ_{c1r}	1000	Kg/m ³
a_{hr}	2	m ²
c_{v1r}	0.006	—
c_{R1r}	0.002354	—
c_{v2r}	0.0011	—
c_{R2r}	0.000134	—
\dot{m}_{s3r}	4.69444	Kg/sec.
\dot{m}_{wor}	105.591	Kg/sec.
\dot{m}_{d2r}	12.75	Kg/sec.
ρ_{wor}	1000	Kg/m ³
ρ_{mr}	1000	Kg/m ³
L_{accr}	13.5	m
r_{accr}	1.75	m



For PI controller

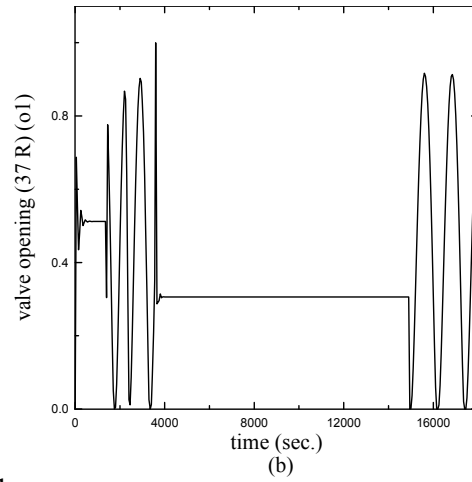
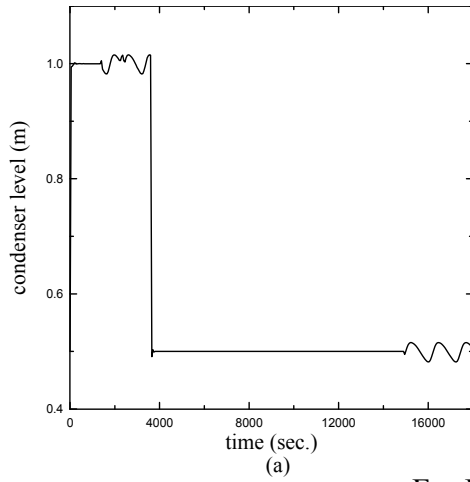


For indirect fuzzy-neural controller

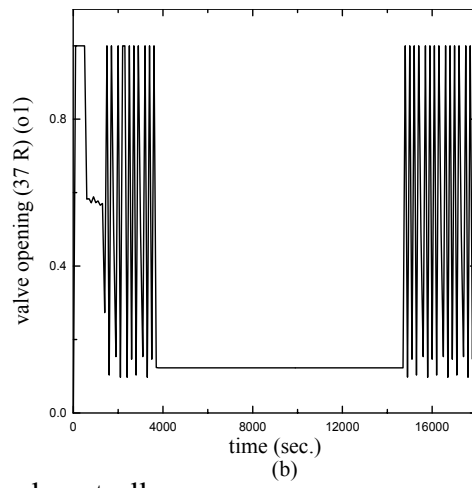
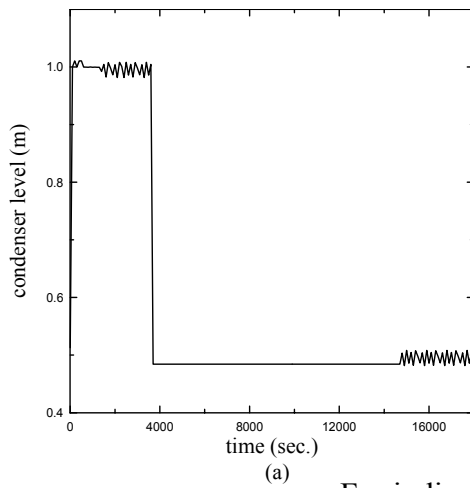


For inverse controller

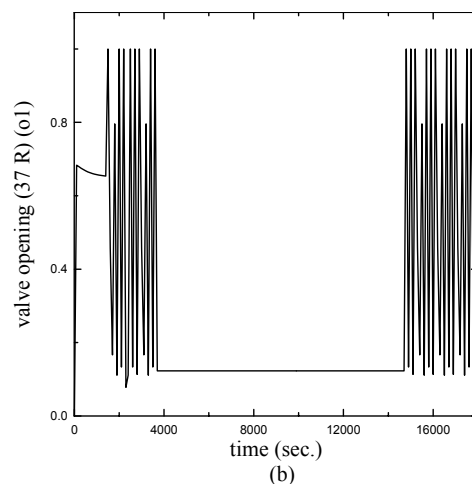
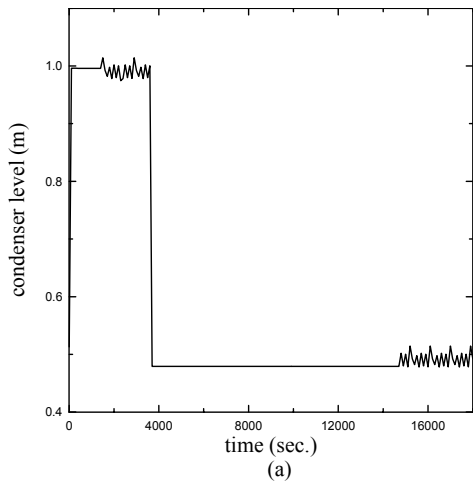
Fig. (17) Changing the (\dot{m}_{s1}) to (40 % load), at $t=2200$ sec.)



For PI controller

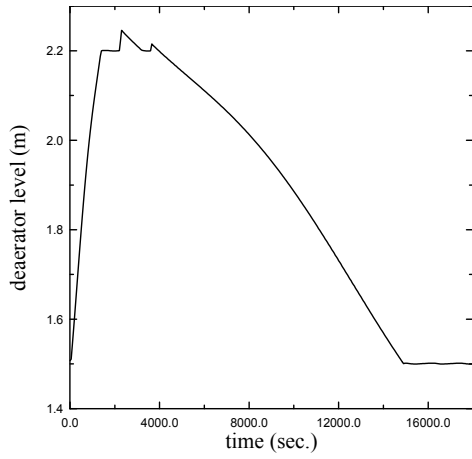


For indirect fuzzy-neural controller

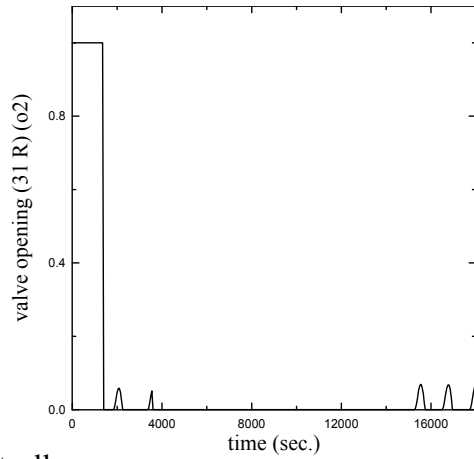


For inverse controller

Fig. (18) Fault occur in the (LPH_s) and removed from the work at t=2200 sec.

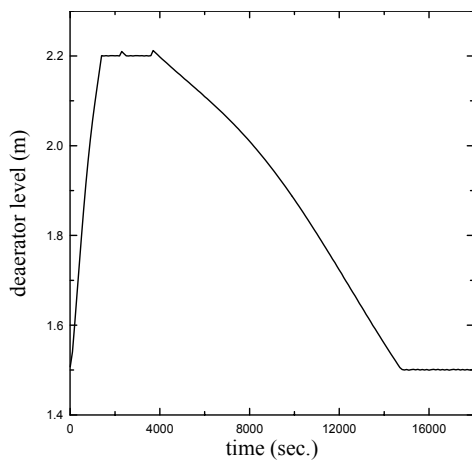


(a)

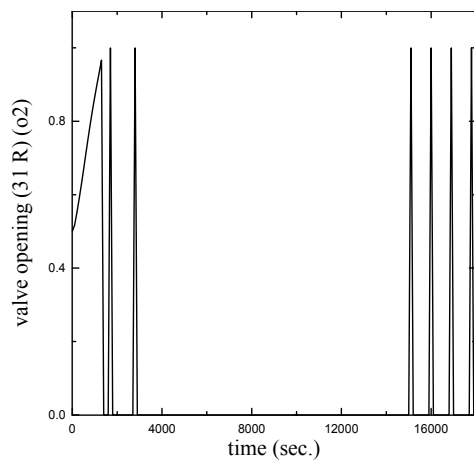


(b)

For PI controller

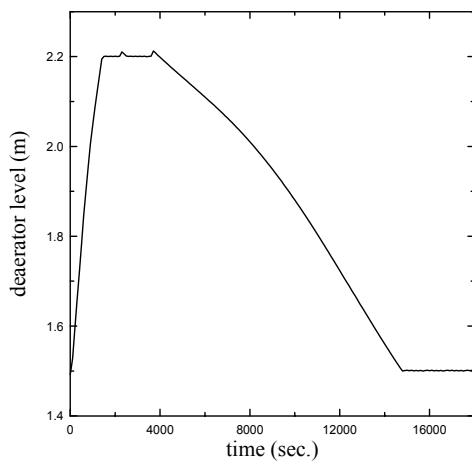


(a)

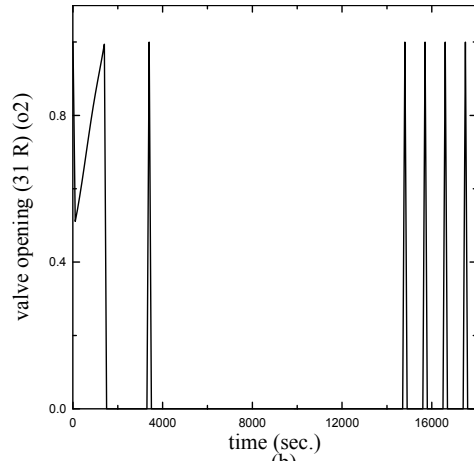


(b)

For indirect fuzzy-neural controller



(a)



(b)

For inverse controller

Fig. (19) Effect of decreasing the (\dot{m}_{wo}) to (70 % load), at $t=2200\text{sec}$.